



OPEN ACCESS

EDITED BY

Ming Wang,
Fudan University, China

REVIEWED BY

Yingfen Wei,
Fudan University, China
Xiaojuan Zhu,
Chinese Academy of Sciences (CAS),
China

*CORRESPONDENCE

A. Jaman,
✉ azminul.jaman@rug.nl
T. Banerjee,
✉ T.Banerjee@rug.nl

SPECIALTY SECTION

This article was submitted to
Nanoelectronics,
a section of the journal
Frontiers in Nanotechnology

RECEIVED 11 December 2022

ACCEPTED 13 February 2023

PUBLISHED 28 February 2023

CITATION

Jaman A, Goossens AS, van Rijn JJJ,
van der Zee L and Banerjee T (2023),
Morphology control of volatile resistive
switching in $\text{La}_{0.67}\text{Sr}_{0.33}\text{MnO}_3$ thin films
on LaAlO_3 (001).

Front. Nanotechnol. 5:1121492.

doi: 10.3389/fnano.2023.1121492

COPYRIGHT

© 2023 Jaman, Goossens, van Rijn, van
der Zee and Banerjee. This is an open-
access article distributed under the terms
of the [Creative Commons Attribution
License \(CC BY\)](https://creativecommons.org/licenses/by/4.0/). The use, distribution or
reproduction in other forums is
permitted, provided the original author(s)
and the copyright owner(s) are credited
and that the original publication in this
journal is cited, in accordance with
accepted academic practice. No use,
distribution or reproduction is permitted
which does not comply with these terms.

Morphology control of volatile resistive switching in $\text{La}_{0.67}\text{Sr}_{0.33}\text{MnO}_3$ thin films on LaAlO_3 (001)

A. Jaman^{1,2*}, A. S. Goossens^{1,2}, J. J. L. van Rijn², L. van der Zee²
and T. Banerjee^{1,2*}

¹Groningen Cognitive Systems and Materials Center, University of Groningen, Groningen, Netherlands,
²Zernike Institute for Advanced Materials, University of Groningen, Groningen, Netherlands

The development of in-memory computing hardware components based on different types of resistive materials is an active research area. These materials usually exhibit analog memory states originating from a wide range of physical mechanisms and offer rich prospects for their integration in artificial neural networks. The resistive states are classified as either non-volatile or volatile, and switching occurs when the material properties are triggered by an external stimulus such as temperature, current, voltage, or electric field. The non-volatile resistance state change is typically achieved by the switching layer's local redox reaction that involves both electronic and ionic movement. In contrast, a volatile change in the resistance state arises due to the transition of the switching layer from an insulator to a metal. Here, we demonstrate volatile resistive switching in twinned LaAlO_3 onto which strained thin films of $\text{La}_{0.67}\text{Sr}_{0.33}\text{MnO}_3$ (LSMO) are deposited. An electric current induces phase transition that triggers resistive switching, close to the competing phase transition temperature in LSMO, enabled by the strong correlation between the electronic and magnetic ground states, intrinsic to such materials. This phase transition, characterized by an abrupt resistance change, is typical of a metallic to insulating behavior, due to Joule heating, and manifested as a sharp increase in the voltage with accompanying hysteresis. Our results show that such Joule heating-induced hysteretic resistive switching exhibits different profiles that depend on the substrate texture along the current path, providing an interesting direction toward new multifunctional in-memory computing devices.

KEYWORDS

volatile memristor, resistive switching, structural twin boundary (TB), neural network, metal to insulator transition (MIT), correlated oxides

1 Introduction

In modern computers, the computation and memory units are separated, leading to a large amount of memory traffic for data retrieval and storage. In contrast, computation in the brain is performed in the memory itself; this co-location of memory and processing reduces latency and energy consumption. Hence, there is a significant interest in developing architectures that mimic brain-like neuronal networks. Hardware components that can emulate brain-like characteristics and possess analog functionalities are promising building blocks for such architectures. A key functionality associated with these devices is resistive

switching that relies on the non-linear electrical transport of the switching material driven by an external stimulus.

In strongly correlated electronic systems (Hwang et al., 2012; Rana et al., 2013; Sulpizio et al., 2014; Roy et al., 2015), correlated oxides are an important material class. Such materials exhibit switching from an insulator to a metal, triggered by various external stimuli such as temperature, pressure, or electric field (Zhang et al., 2020). Mott insulators such as VO_2 , V_2O_3 , and NbO_2 are examples of such materials (Stoliar et al., 2014; Kumar et al., 2017; Valmianski et al., 2018; Kalcheim et al., 2020). When electrically triggered, they undergo a change in resistance, spanning over an order of magnitude, changing from an insulating behavior below its critical temperature (T_C) to a metallic state above it (Imada et al., 1998), rendering them useful for volatile resistive switching applications. Such switching of resistive states between two phases involves a structural transition that happens at high operational temperatures. These materials are reported to be quite efficient for mimicking certain brain functionalities, including integrate and fire neurons and short-term memory, and involve the requirement of high temperature to drive the structural transformation to derive the distinct resistive phases (Liu et al., 2016; Kumar et al., 2017). In this context, the quest for material systems that exhibit volatile resistive switching but not involving any structural transition is a promising research direction.

In this work, we demonstrate volatile resistive switching in strained thin films of $\text{La}_{0.7}\text{Sr}_{0.3}\text{MnO}_3$ (LSMO) deposited on LaAlO_3 (LAO) substrates. LSMO is a mixed-valence doped material in the $\text{La}_{1-x}\text{Sr}_x\text{MnO}_3$ manganite family, displaying a wide range of electronic and magnetic phases (Izyumskaya et al., 2009) depending on the doping and ionic radii of the divalent cations. Thin films of LSMO are metallic ferromagnets below their T_C of approximately 370 K and undergo transition to insulating paramagnets above this temperature. In our earlier works (Burema et al., 2019; Burema and Banerjee, 2021), we have demonstrated that compressively strained thin films of $\text{La}_{0.7}\text{Sr}_{0.3}\text{MnO}_3$ on a LaAlO_3 substrate with twin domains lead to the coexistence of different magnetically ordered phases, as revealed from magnetization and electronic transport measurements. This was ascribed to the strain-induced Jahn–Teller distortion that favors $d_{3z^2-r^2}$ orbitals over $d_{x^2-y^2}$ orbitals at such compressively strained interfaces. The coupling between the electronic and magnetic phases in such strained films, without any accompanying structural transition, makes them good candidates for volatile resistive switching operation. In this work, we electrically induce resistive switching, by Joule heating, in 10-nm strained LSMO films deposited on textured substrates of LAO. We observe volatile resistive switching in LSMO and use the morphology of twin planes in LAO to capture the nature of resistive switching across different connection pathways. By designing contacts that intersect differently oriented twin planes, we demonstrate abrupt changes in the film resistance, with accompanying hysteresis at temperatures close to the phase transition. We foresee that volatile and non-volatile switching can be realized in such LSMO films deposited on LAO by a careful choice of both the operating temperature and the magnitude of the input stimuli. Such features are useful for charge-based oscillators that can mimic the spiking behavior of neurons in the human brain, relevant for in-memory computing applications.

2 Materials and methods

LSMO films of 10 nm thickness were grown on textured $(001)_{pc}$ oriented LAO substrates using pulsed laser deposition (PLD). A KrF excimer laser (248 nm) was focused onto an LSMO target with a laser fluence of 2 J/cm^2 and a repetition rate of 1 Hz. During the growth, the substrate temperature was kept at 750°C , at an oxygen pressure of 0.35 mbar. After deposition, the films were cooled to room temperature at an oxygen pressure of 100 mbar. Different X-ray diffraction techniques, including X-ray reflectivity (XRR) and reciprocal space mapping (RSM), were used to infer the structure, thickness, and strain of the deposited films. Temperature-dependent magnetic measurements, using a superconducting quantum interference magnetometer (SQUID), were carried out to determine the magnetic phase of the films. For electrical measurements, Ti/Au gold contacts were deposited at the four corners of the film using UV-lithography and electron beam evaporation. Current- and voltage-controlled resistive switching measurements were performed using a Keithley 2451 source meter.

3 Results

The growth of the films is monitored using the high-energy electron diffraction (RHEED) technique. The observed diffraction spots at (00), (01), and (0 $\bar{1}$) and RHEED oscillations are shown in Supplementary Figure S1A. The intensity distribution of the central spot over time suggests a 2D layer-by-layer growth, and their streaky nature suggests the formation of domains (Haeni et al., 2000). Figure 1A shows the θ - 2θ scan with the signature Bragg reflection peak of LSMO (002) at 46.4° , confirming the growth of LSMO on the substrate. The out-of-plane lattice parameter is calculated to be 3.90 Å, whereas the bulk lattice parameter of LSMO is 3.88 Å. This suggests an out-of-plane elongation of the MnO_6 octahedra with a strain percentage of 0.51%. Figure 1B shows the 3D RSM around the (103) crystallographic peak of the substrate and the film, confirming the epitaxial growth of LSMO on the LAO substrate. The two peaks are aligned with the same in-plane lattice parameter of 3.79 Å, indicating that the film is strained with an in-plane strain percentage of $\sim -0.25\%$. A slight smearing of the film peak along the upper left shoulder is observed, which indicates that the crystalline direction is not uniform throughout the film due to the presence of twin boundary domains. $\text{La}_{0.7}\text{Sr}_{0.3}\text{MnO}_3$ is a ferromagnetic metal below its Curie temperature, T_C . To characterize the magnetic properties, the zero-field-cooled (ZFC) magnetization (M) dependence on temperature (T) was measured at a running field of 50 Oersted, along the in-plane direction, while warming up the film. Figure 2A shows that the magnetization follows the Curie–Weiss law, with ferromagnetic behavior at low temperatures (below T_C) and paramagnetic behavior above T_C . The T_C is found to be 325 K, which is determined from the first derivative of the magnetization with respect to temperature, as shown on the right axis of Figure 2B. The sheet resistance of the film was determined in the van der Pauw configuration. The dependence of resistance (R) on temperature (T) was extracted from the voltage drop recorded across the contacts by applying a direct current (dc) of 1 μA . The shape of the R vs T curve, as shown in Figure 2C, indicates that the film shows metallic behavior at low temperatures

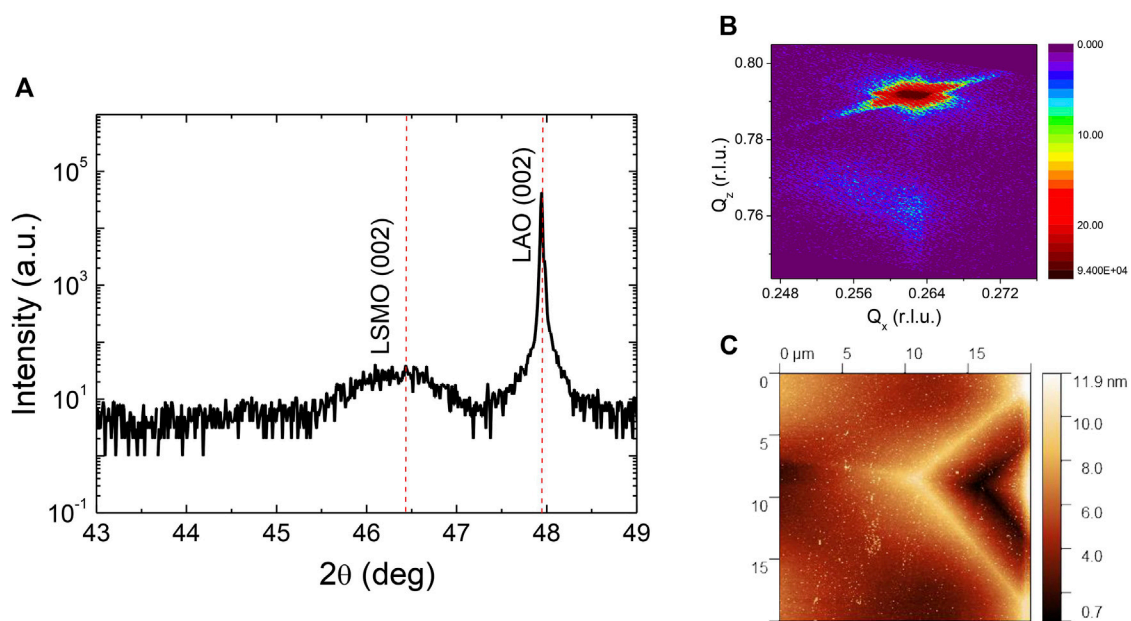


FIGURE 1 (A) XRD pattern of LSMO/LAO thin film showing a smooth and epitaxial growth of ~ 24 unit cells. This thickness is in close correspondence to that determined by *in situ* RHEED (Supplementary Figure S1A) and by XRR (Supplementary Figure S1B). The corresponding angles for LSMO (002) and LAO (002) are indicated by the red dotted lines. (B) Reciprocal space map of the (103) Bragg reflection peak of LAO and LSMO shows that the grown film is elongated out of the plane direction to match the lattice parameter of the LAO substrate. (C) AFM image shows structural twin domains of the LAO substrate.

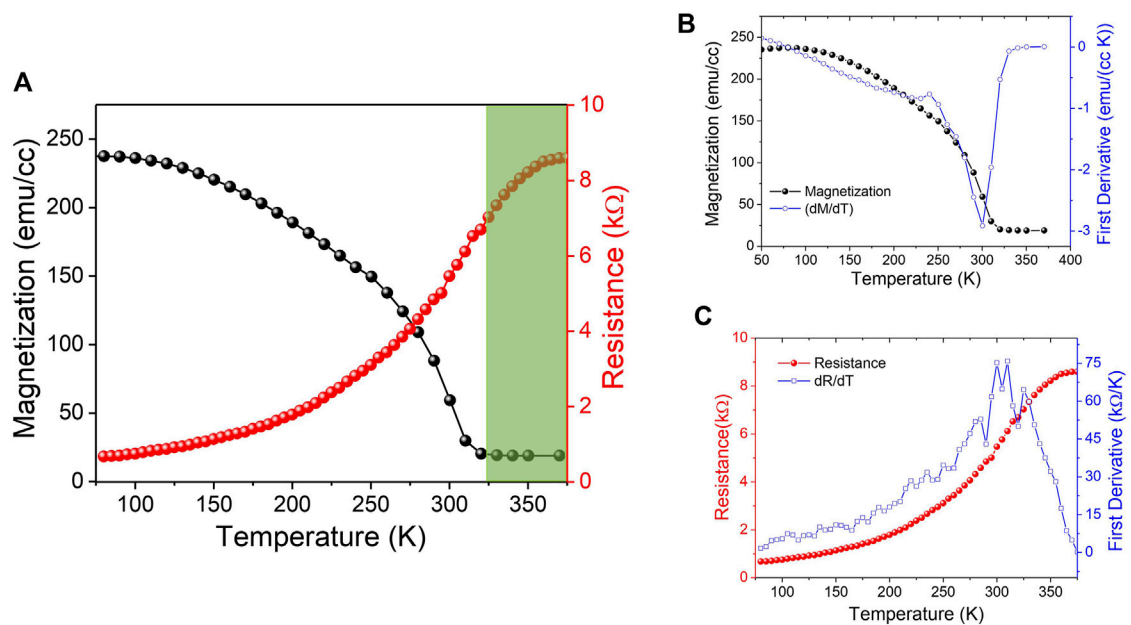


FIGURE 2 (A) Magnetization (black) and resistance (red) vs temperature. The region in white is the ferromagnetic metallic regime, and the green-shaded region is the paramagnetic insulating regime. (B) Zero-field-cooled magnetization vs temperature plot obtained with a running magnetic field of 50 Oe shows that the film follows the Curie–Weiss law exhibiting ferromagnetic behavior up to $T_C \sim 325$ K, determined by the slope change (dM/dT) with respect to temperature. (C) Zero-field-cooled resistivity vs temperature dependence obtained with a fixed direct current of 1 μA in the van der Pauw configuration, which shows metallic behavior up to $T_{MIT} \sim 325$ K, determined by the slope change (dR/dT) with respect to temperature.

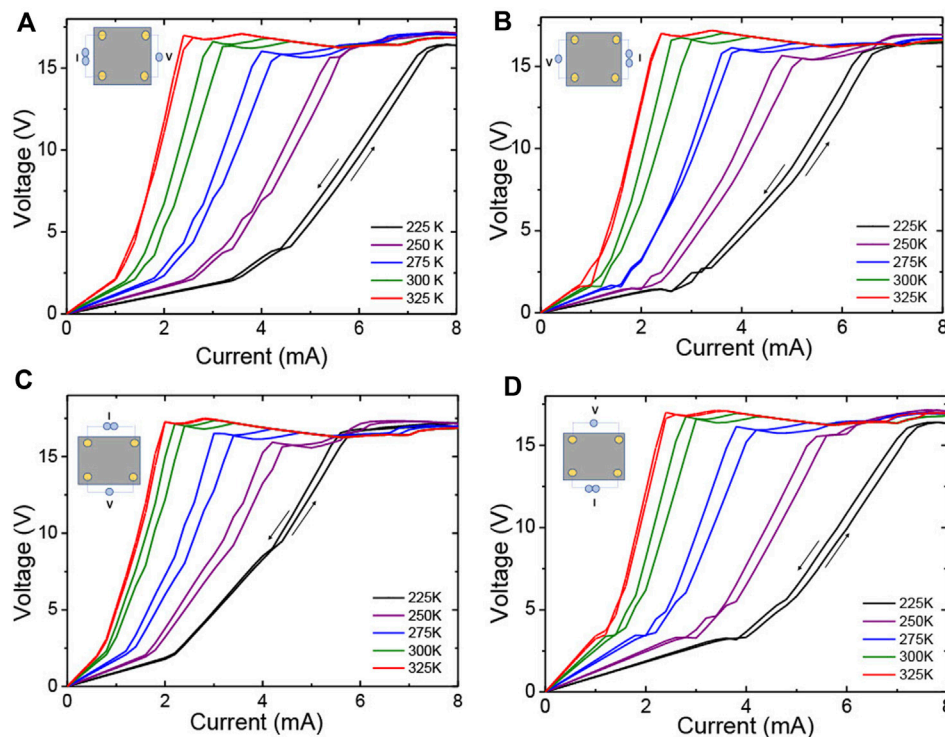


FIGURE 3

Current-controlled hysteretic resistive switching behavior at different temperatures shown from 225 K to 325 K for (A) left-vertical, (B) right-vertical, (C) top-horizontal, and (D) bottom-horizontal directions. Left (right)-vertical refers to current sourcing in the vertical direction through a pair of left or right contacts. Current sourcing in the horizontal direction using a pair of top or bottom contacts is referred to as top-horizontal or bottom-horizontal. As the temperature increases and approaches T_{MIT} , the current needed for switching to occur decreases establishing the Joule heating origin of the switching.

and insulating behavior at high temperatures. The metal-to-insulator transition temperature (T_{MIT}) is found to be 325 K, which is determined from the first derivative of R with T , as shown on the right axis of Figure 2C. The strong correlation between T_C and T_{MIT} shows that the electronic and magnetic properties are coupled, as shown in Figure 2A. This arises due to the double exchange interaction (Dörr, 2006), which promotes parallel alignment of the manganese (Mn) magnetic moments by enhancing the hopping probability of the itinerant electrons from Mn^{3+} sites to adjacent Mn^{4+} sites, leading to a low resistance state. Close to the transition temperature, the thermal energy destabilizes this parallel alignment by reducing the hopping probabilities of the itinerant electrons, yielding a high resistance state in the paramagnetic state (Tokura and Tomioka, 1999; Haghiri-Gosnet and Renard, 2003; Štrbík et al., 2014).

Ti/Au gold contacts were deposited at the four corners of the sample for resistive switching experiments. One pair of contact is chosen at each edge, to source the current, and another pair is used to sense the voltage at the opposite edge. This configuration enables us to probe the entire surface of the film in four different combinations and directions. Voltage (V) vs current (I) sweeps were taken in all directions at different temperatures, as shown in Figure 3. Each graph shows a transition from a linear to non-linear transport across the entire substrate with increasing current. At 225 K, below T_{MIT} , the measured voltage is linear up to 3.25 mA (left-vertical),

2.27 mA (right-vertical), 2 mA (top-horizontal), and 3.62 mA (bottom-horizontal). This is followed by an abrupt change in the slope of the resistance as the current is further increased. This is associated with the transition of the film from a ferromagnetic low-resistance state to a paramagnetic high-resistance state accompanied by a small hysteresis due to Joule heating. A further slope change is observed for higher currents, after which the measured voltage levels off near compliance voltage. The film returns to its initial low-resistance state when the sourced current is ramped to zero, indicative of volatile resistance behavior. Furthermore, as the temperature is increased closer to T_{MIT} , the threshold current for switching decreases, as shown in Figure 3. This is consistent with the associated metal-to-insulator transition, as observed in the $R-T$ measurements (shown in Supplementary Figure S6B). Similarly, the voltage-controlled sweeps (shown in Supplementary Figure S6A) show a rapid increase in current beyond a threshold voltage. Thus, in both measurement types, we identify distinct regimes of changes in resistive states across the entire substrate at each temperature. The corresponding $I-V$ curves measured in all directions show a systematic variation with increasing temperature (Figure 3) (See Supplementary Figure S5 and Supplementary Figure S13). Furthermore, we have carried out similar measurements on different twinned substrates and also on LSMO films of different thicknesses (Supplementary Figures S11, S12). Schematics of the current conduction path along different directions of the films

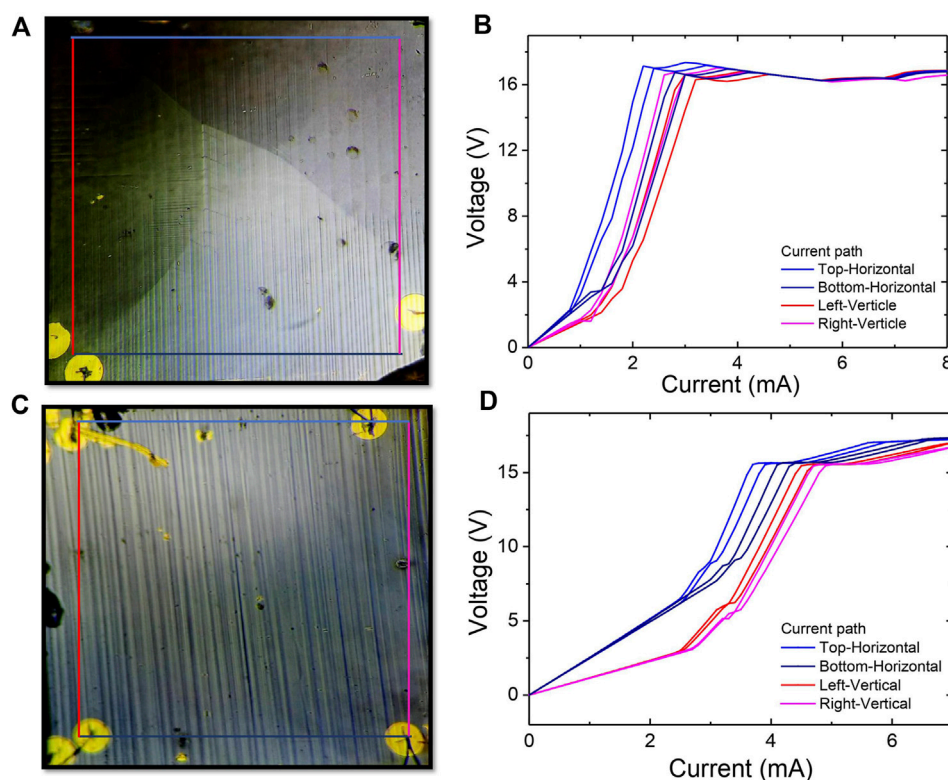


FIGURE 4

Optical microscopic image of an LSMO thin film grown on a 5 mm × 5 mm (A) inhomogeneously distributed vertical and horizontal twinned domain LAO substrate and (C) homogeneously distributed twinned domains along the vertical direction of the LAO substrate. The corresponding current vs voltage sweeps of (A) and (C) at 300 K are shown in (B) and (D).

deposited on two distinctly textured LAO substrates are shown in Figures 4A, C. Current vs voltage sweeps in different directions are shown in Figures 4B, D for the two substrates (See Supplementary Figure S9). The optical image of the two substrates shows that the twin domain density, orientation, and homogeneity are different for substrates A and B. The distribution of twin domains influences the magnitude of the current needed to drive the LSMO phase transition, resulting in differences between the two samples and along the different directions as shown in Figures 4A, C. Furthermore, we see that the resistance post-switching and the current at which the voltage (~ 15 V) levels off are also different for the vertical and horizontal directions. In uniformly terminated substrates, such as in SrTiO₃, it is unusual for the dc electrical resistance of LSMO thin films to depend on the measurement direction (Oliveira et al., 2020). In twinned substrates of LAO, however, our findings show that the density, as well as the orientation of the twin domains, yields differences in the resistance when measured along or across the twin boundaries, induced by local changes in strain and electronic properties of the LSMO films.

4 Discussion

In manganites, non-volatile resistive phase transitions involving structural and stoichiometric changes are well studied (Asamitsu et al., 1997; Kalkert et al., 2011; Jeon et al., 2021). In LSMO, for example, it

has been shown that oxygen vacancy-driven resistive phase transitions occur and are accompanied by structural transformations from a perovskite to a brownmillerite phase (Brockman et al., 2014). Volatile resistive switching, on the other hand, utilizes the strong coupling between electronic and magnetic phases (Salev et al., 2021) and does not involve structural phase transitions (See Supplementary Figure S3 and Supplementary Figure S8).

In our case, we determine the resistive switching to be volatile in nature and related to a metal-to-insulator transition in LSMO. We demonstrate electrical control of this transition in Figures 3, 4. Joule heating induces a local increase in temperature, triggering a phase transition when the film temperature locally exceeds T_{MIT} . This is manifested as an abrupt increase in voltage across the entire film and measured by a pair of contacts positioned across different corners of the substrate. The film returns to its original state when the current is ramped down, thus representing a volatile change in the resistance state (Supplementary Figure S10A shows no film degradation up to 100 cycles). By increasing the measurement temperature and bringing it closer to T_{MIT} , the current required for the transition to occur is lowered (Figures 3, 4 and Supplementary Figure S4). Due to the substrate's morphology involving the random orientation of twin domains, the resistance is expected to depend on whether it is measured across the horizontal or vertical contacts. Rhombohedral wedge-shaped twin domains are frequently observed in the plane of such LAO substrates (shown in Figure 1C and Supplementary Figure S2A). Although these domains are unidirectional, the

spacing and angle between the twin boundaries are not equal in all directions. This creates differences in the strain environment, leading to a distribution of ferromagnetic metallic phases with small differences in the oxygen of the MnO_6 octahedra, resulting in a complex structure. In such a network, the electrical conductivity is distinctly controlled by the hopping probability of the itinerant d electrons from one Mn site to another, which varies locally due to local differences in the Mn-O-Mn bond angle across or along the twin domains as shown in Figure 3. The accompanying hysteresis results from the lower current needed to maintain the same voltage during retrace. Bare LAO substrates were measured as shown in Supplementary Figure S7; in this case, the resistance is found to be high, and no hysteretic behavior is observed.

5 Conclusion

The current-induced Joule heating-triggered resistive switching that our experiments demonstrate is unlike i) the widely studied Mott insulators that transform to a metallic state from an insulating state by forming a conducting filament parallel to the current flow or ii) LSMO films on well-ordered substrates, such as STO, where the switch from a metallic to an insulating state happens by the formation of a transverse barrier perpendicular to the current flow (Salev et al., 2021). By utilizing a substrate possessing twin domains, we are able to build a complex resistive structure based on the electronic phase transition. The local variations in strain results in a distribution of coexisting ferromagnetic metallic states. Given that each of these phases can transition to a paramagnetic phase at a nominally different threshold current value, this further increases the number of states in the complex structure. Additional tuning of the phase transition temperature is possible by controlling the epitaxial strain through film thickness, which allows control over the switching energy. Both volatile and non-volatile switching can be realized in the same film depending on the proximity of the operating temperature to the transition temperature and on the magnitude of the input stimuli. Contrary to the existing Mott-based memories, no structural transition is associated with the resistive phase transition demonstrated here, making the switching highly stable over a large number of cycles. Our work opens new possibilities for studying such coexisting states using nanoscale probing techniques (Banerjee et al., 2005) as well as for incorporating other transition metal oxides that can provide non-linear strain coupling due to their (pseudo)cubic crystal structure, useful for brain-inspired computing structures. These structures may be exploited in emergent complex learning functionalities ranging from shortest path optimization (Pershin and Di Ventra, 2013) to associative memory (Diaz-Alvarez et al., 2020) or providing a framework for reservoir computing applications.

References

- Asamitsu, A., Tomioka, Y., Kuwahara, H., and Tokura, Y. (1997). Current switching of resistive states in magnetoresistive manganites. *Nature* 388, 50–52. doi:10.1038/40363
- Banerjee, T., Haq, E., Siekman, M., Lodder, J., and Jansen, R. (2005). Ballistic hole emission microscopy on metal-semiconductor interfaces. *IEEE Trans. Magnetics* 41, 2642–2644. doi:10.1109/TMAG.2005.854738

Data availability statement

The original contributions presented in the study are included in the article/Supplementary Material, further inquiries can be directed to the corresponding authors.

Author contributions

AJ and TB conceived the idea, AJ and AG planned the different experiments including fabrication of the devices, JvR helped with the measurements and data analysis along with LvdZ. The paper was written by AJ and TB with useful input from all authors.

Acknowledgments

The authors would like to thank all members of the Spintronics of Functional Materials group at the University of Groningen, including P. Zhang, S. Chen, and A. Das, for useful scientific discussions. Thin film growth and device fabrication were realized using NanoLab NL facilities. The authors acknowledge technical support from J. Baas, J. G. Holstein, and H. H. de Vries.

Conflict of interest

The authors declare that the research was conducted in the absence of any commercial or financial relationships that could be construed as a potential conflict of interest.

Publisher's note

All claims expressed in this article are solely those of the authors and do not necessarily represent those of their affiliated organizations, or those of the publisher, the editors and the reviewers. Any product that may be evaluated in this article, or claim that may be made by its manufacturer, is not guaranteed or endorsed by the publisher.

Supplementary material

The Supplementary Material for this article can be found online at: <https://www.frontiersin.org/articles/10.3389/fnano.2023.1121492/full#supplementary-material>

- Brockman, J. S., Gao, L., Hughes, B., Rettner, C. T., Samant, M. G., Roche, K. P., et al. (2014). Subnanosecond incubation times for electric-field-induced metallization of a correlated electron oxide. *Nat. Nanotechnol.* 9, 453–458. doi:10.1038/nnano.2014.71

- Burema, A. A., van Rijn, J. J., and Banerjee, T. (2019). Temperature dependence of the magnetization of $\text{La}_{0.67}\text{Sr}_{0.33}\text{MnO}_3$ thin films on LaAlO_3 . *J. Vac. Sci. Technol. A Vac. Surfaces, Films* 37, 021103. doi:10.1116/1.5085933

- Burema, A., and Banerjee, T. (2021). Temperature-dependent periodicity halving of the in-plane angular magnetoresistance in $\text{LaO}_x/\text{SrTiO}_3/\text{SrTiO}_3$ thin films on LaAlO_3 . *Appl. Phys. Lett.* 119, 011901. doi:10.1063/5.0051629
- Diaz-Alvarez, A., Higuchi, R., Li, Q., Shingaya, Y., and Nakayama, T. (2020). Associative routing through neuromorphic nanowire networks. *AIP Adv.* 10, 025134. doi:10.1063/1.5140579
- Dörr, K. (2006). Ferromagnetic manganites: Spin-polarized conduction versus competing interactions. *J. Phys. D Appl. Phys.* 39, R125–R150. doi:10.1088/0022-3727/39/7/r01
- Haeni, J., Theis, C. D., and Schlom, D. G. (2000). Rheed intensity oscillations for the stoichiometric growth of SrTiO_3 thin films by reactive molecular beam epitaxy. *J. Electroceramics* 4, 385–391. doi:10.1023/a:1009947517710
- Haghiri-Gosnet, A., and Renard, J. (2003). Cmr manganites: Physics, thin films and devices. *J. Phys. D Appl. Phys.* 36, R127–R150. doi:10.1088/0022-3727/36/8/201
- Hwang, H. Y., Iwasa, Y., Kawasaki, M., Keimer, B., Nagaosa, N., and Tokura, Y. (2012). Emergent phenomena at oxide interfaces. *Nat. Mater.* 11, 103–113. doi:10.1038/nmat3223
- Imada, M., Fujimori, A., and Tokura, Y. (1998). Metal-insulator transitions. *Rev. Mod. Phys.* 70, 1039–1263. doi:10.1103/revmodphys.70.1039
- Izyumskaya, N., Alivov, Y., and Morkoc, H. (2009). Oxides, oxides, and more oxides: High- κ oxides, ferroelectrics, ferromagnetics, and multiferroics. *Crit. Rev. Solid State Mater. Sci.* 34, 89–179. doi:10.1080/10408430903368401
- Jeon, J., Jung, J., and Chow, K. (2021). Electronic phase separation induced non-volatile bi-polar resistive switching in spatially confined manganite microbridges. *J. Phys. D Appl. Phys.* 54, 315002. doi:10.1088/1361-6463/abf7
- Kalcheim, Y., Camjayi, A., Del Valle, J., Salev, P., Rozenberg, M., and Schuller, I. K. (2020). Non-thermal resistive switching in Mott insulator nanowires. *Nat. Commun.* 11, 2985–2989. doi:10.1038/s41467-020-16752-1
- Kalkert, C., Krispeneit, J.-O., Esseling, M., Lebedev, O. I., Moshnyaga, V., Damaschke, B., et al. (2011). Resistive switching at manganite/manganite interfaces. *Appl. Phys. Lett.* 99, 132512. doi:10.1063/1.3643425
- Kumar, S., Wang, Z., Davila, N., Kumari, N., Norris, K. J., Huang, X., et al. (2017). Physical origins of current and temperature controlled negative differential resistances in NbO_2 . *Nat. Commun.* 8, 658. doi:10.1038/s41467-017-00773-4
- Liu, X., Li, S., Nandi, S. K., Venkatachalam, D. K., and Elliman, R. G. (2016). Threshold switching and electrical self-oscillation in niobium oxide films. *J. Appl. Phys.* 120, 124102. doi:10.1063/1.4963288
- Oliveira, F., Cipriano, R., da Silva, F., Romão, E., and Dos Santos, C. (2020). Simple analytical method for determining electrical resistivity and sheet resistance using the van der Pauw procedure. *Sci. Rep.* 10, 16379. doi:10.1038/s41598-020-72097-1
- Pershin, Y. V., and Di Ventra, M. (2013). Self-organization and solution of shortest-path optimization problems with memristive networks. *Phys. Rev. E* 88, 013305. doi:10.1103/physreve.88.013305
- Rana, K. G., Yajima, T., Parui, S., Kemper, A. F., Devereaux, T. P., Hikita, Y., et al. (2013). Hot electron transport in a strongly correlated transition-metal oxide. *Sci. Rep.* 3, 1274. doi:10.1038/srep01274
- Roy, S., Autieri, C., Sanyal, B., and Banerjee, T. (2015). Interface control of electronic transport across the magnetic phase transition in $\text{SrRuO}_3/\text{SrTiO}_3$ heterointerface. *Sci. Rep.* 5, 15747. doi:10.1038/srep15747
- Salev, P., Fratino, L., Sasaki, D., Berkoun, R., Del Valle, J., Kalcheim, Y., et al. (2021). Transverse barrier formation by electrical triggering of a metal-to-insulator transition. *Nat. Commun.* 12, 5499. doi:10.1038/s41467-021-25802-1
- Stoliar, P., Rozenberg, M., Janod, E., Corraze, B., Tranchant, J., and Cario, L. (2014). Nonthermal and purely electronic resistive switching in a Mott memory. *Phys. Rev. B* 90, 045146. doi:10.1103/physrevb.90.045146
- Štrbík, V., Reiffers, M., Dobročka, E., Šoltýs, J., Španková, M., and Chromik, Š. (2014). Epitaxial LaMO_3 thin films with correlation of electrical and magnetic properties above 400 K. *Appl. Surf. Sci.* 312, 212–215. doi:10.1016/j.apsusc.2014.04.045
- Sulpizio, J. A., Ilani, S., Irvin, P., and Levy, J. (2014). Nanoscale phenomena in oxide heterostructures. *Annu. Rev. Mater. Res.* 44, 117–149. doi:10.1146/annurev-matsci-070813-113437
- Tokura, Y., and Tomioka, Y. (1999). Colossal magnetoresistive manganites. *J. magnetism magnetic Mater.* 200, 1–23. doi:10.1016/s0304-8853(99)00352-2
- Valmianski, I., Wang, P., Wang, S., Ramirez, J. G., Guénon, S., and Schuller, I. K. (2018). Origin of the current-driven breakdown in vanadium oxides: Thermal versus electronic. *Phys. Rev. B* 98, 195144. doi:10.1103/physrevb.98.195144
- Zhang, H.-T., Panda, P., Lin, J., Kalcheim, Y., Wang, K., Freeland, J. W., et al. (2020). Organismic materials for beyond von Neumann machines. *Appl. Phys. Rev.* 7, 011309. doi:10.1063/1.5113574